Numerical back-analysis and effective prediction of the long-term settlement of airport high fill

Jian Huang [i, ii)], Ting Luo* [iii)], Hongye Yan [iv)], Feng Chen [v)], Qianli Zhang [vi)]

i) Ph.D Student, School of Transportation Science and Engineering, Beihang University, 37, Xueyuan Road, Beijing, 100191, China.
ii) Ph.D Student, State Key Laboratory of High-speed Railway Track Technology, 2, Daliushu Road, Haidian District, Beijing, 100081, China.
iii) Professor, School of Transportation Science and Engineering, Beihang University, 37, Xueyuan Road, Beijing, 100191, China.
iv) Associate professor, Academy of Railway Sciences Corporation Limited, 2, Daliushu Road, Haidian District, Beijing, 100081, China.
v) Professor, Academy of Railway Sciences Corporation Limited, 2, Daliushu Road, Haidian District, Beijing, 100081, China.
vi) Professor, Academy of Railway Sciences Corporation Limited, 2, Daliushu Road, Haidian District, Beijing, 100081, China.

ABSTRACT

The long-term settlement of high fill is large, which may affect the practical application of engineering. Therefore, it is crucial to study the calculation method and effective prediction range of long-term settlement. In this paper, a numerical back-analysis platform based on genetic algorithm and time-dependent UH model is established. It is verified that the numerical calculation based on time-dependent UH model is applicable to predict the long-term settlement by the settlement monitoring data of the high fill in Chengde Airport, Hebei province. The effective prediction interval method of long-term settlement is proposed and the corresponding calculation equation is derived. According to the existing measured data interval t_m, the equation can be used to quantitatively calculate the effective prediction interval t_e under a specific settlement error limit. At last, the effective prediction interval is calculated through the monitoring data of the high fill in Chengde Airport.

Keywords: high fill, long-term settlement, time-dependent UH model, back-analysis, effective prediction interval

1 INTRODUCTION

High fill airports are widely distributed all over the world. Especially, they are more and more constructed in recent years in China. Large volume and high height determine that the high-fill airport will produce long-term settlement under the action of high gravity stress after the completion of filling. To avoid excessive and differential settlement, runway, apron and other structures should be constructed after the fill is stable. Therefore, it is of great significance to track, monitor and predict the long-term settlement of airport high fill.

There are three main prediction methods for long-term settlement. The first is the curve fitting method commonly used in practical engineering. It's simple and practical. This method has a variety of commonly formulas, such as the three-point method (Zeng and Yang 1959), the hyperbolic method (Sridharan et al. 1987) and so on. Yao et al. (2018a) proposed a practical creep settlement algorithm suitable for long-term settlement of high fill, which has the characteristics of few parameters and clear physical significance. The second is system analysis method, which mainly includes the grey model method (Liu and Yang 2015) and the artificial neural network prediction model method (Peng et al. 2005). The third is numerical calculation, such as finite element method and finite difference method. Constitutive model is very important in numerical calculation. Yao et al. (2013, 2015) introduced the equivalent time into the current yield function of the UH model, established the time-dependent UH model that can simultaneously

describe the soil's over-consolidation and rate effect.

For long-term settlement, the prediction curve determined by numerical calculation cannot accurately predict the settlement at any time. Yao et al. (2018b) preliminarily discussed the determination of the effective prediction range through the creep practical algorithm. In fact, the closer the monitoring time is, the more accurate the prediction results will be; the farther from the monitoring time, the larger the prediction error. Then, under a certain settlement error limit, how long it can be effectively predicted (i.e. effective prediction interval) is an issue worth exploring.

This paper introduces the time-dependent UH model, and builds a back analysis platform based on the multi-island genetic algorithm and the time-dependent UH model. Then a method to calculate effective prediction interval for long-term settlement is proposed. Finally, according to the settlement monitoring data of Chengde Airport high fill, long-term settlement under different monitoring data intervals are predicted, and the corresponding effective prediction intervals are calculated.

2 THE TIME-DEPENDENT UH MODEL

Compared with the modified Cam-clay model, the UH model can describe shear contraction and dilatation, strain hardening and softening as well as stress-path-dependency of saturated over-consolidated clay soil (Yao et al. 2008a; Yao et al. 2008b; Yao et al. 2009; Yao and Zhou 2013; Gao et al. 2010; Guo et al. 2013). The equivalent time is introduced into the current yield function of the UH model, the effect of time on soil is considered, and the relationship between time and over-consolidation ratio is established to realize creep calculation.

The stress-strain relationship of the time-dependent UH model in the *p*-*q* plane is shown in Eq. (1). For more derivation process about the time-dependent UH model, refer to the previous publications of one of the authors (Yao et al. 2013, 2014).

$$\begin{bmatrix} \mathrm{d}p + B_1 \mathrm{d}t \\ \mathrm{d}q + B_2 \mathrm{d}t \end{bmatrix} = \begin{bmatrix} K \cdot A_1 & 3KG \cdot A_2 \\ 3KG \cdot A_2 & 3G \cdot A_3 \end{bmatrix} \begin{bmatrix} \mathrm{d}\varepsilon_\mathrm{v} \\ \mathrm{d}\varepsilon_\mathrm{d} \end{bmatrix} \tag{1}$$

where $K = E \big/ 3(1-2\nu)$ is the elastic bulk modulus and $G = E \big/ 2(1+\nu)$ is the elastic shear modulus; A_1, A_2 and A_3 are different influencing factors of stresses; B_1 and B_2 are different influencing factors of time.

The expression of A_1, A_2, A_3, B_1 and B_2 can be given as:

$$A_1 = \frac{\left(M_\mathrm{f}^4 - \eta^4\right) p + 12Gc_\mathrm{p}\eta^2}{\left(M_\mathrm{f}^4 - \eta^4\right) p + 12Gc_\mathrm{p}\eta^2 + Kc_\mathrm{p}\left(M^2 - \eta^2\right)^2} \tag{2}$$

$$A_2 = \frac{-2c_\mathrm{p}\left(M^2 - \eta^2\right)\eta}{\left(M_\mathrm{f}^4 - \eta^4\right) p + 12Gc_\mathrm{p}\eta^2 + Kc_\mathrm{p}\left(M^2 - \eta^2\right)^2} \tag{3}$$

$$A_3 = \frac{\left(M_\mathrm{f}^4 - \eta^4\right) p + Kc_\mathrm{p}\left(M^2 - \eta^2\right)^2}{\left(M_\mathrm{f}^4 - \eta^4\right) p + 12Gc_\mathrm{p}\eta^2 + Kc_\mathrm{p}\left(M^2 - \eta^2\right)^2} \tag{4}$$

$$B_1 = \frac{pc_\mathrm{p}\omega K\left(M^4 - \eta^4\right)}{\left(M_\mathrm{f}^4 - \eta^4\right) p + 12Gc_\mathrm{p}\eta^2 + Kc_\mathrm{p}\left(M^2 - \eta^2\right)^2} \tag{5}$$

$$B_2 = \frac{6qc_\mathrm{p}\omega G\left(M^2 + \eta^2\right)}{\left(M_\mathrm{f}^4 - \eta^4\right) p + 12Gc_\mathrm{p}\eta^2 + Kc_\mathrm{p}\left(M^2 - \eta^2\right)^2} \tag{6}$$

where ω is expressed as:

$$\omega = \frac{\beta}{\lambda - \kappa} \frac{M_\mathrm{f}^4}{M^4} R^{\frac{\lambda - \kappa}{\beta}} \tag{1}$$

where $C_{\alpha e}$ is the coefficient of secondary consolidation in e-ln(t+1) space; λ is the slope of normal compression line in e-ln$p$ space; κ is the slope of elastic rebound line in e-ln$p$ space; M is the stress ratio of the critical state and the characteristic state; M_f is potentially damaging stress ratio; η is effective stress ratio (η=q/p'); R is the parameter of over-consolidated.

Compared with the modified Cam-clay model, the time-dependent UH model only adds a parameter called viscosity coefficient β, and all parameters can be determined by laboratory tests. Table 1 is listed the parameters and corresponding physical significance of time-dependent UH model.

Table 1. Parameters of time-dependent UH model.

Parameter	Physical significance
M	the stress ratio of the critical state and the characteristic state
λ	the slope of normal compression line
κ	the slope of elastic rebound line
ν	the Poisson's ratio
N	pore ratio on the instant normal compression line when p=1kpa
e_0	initial pore ratio
c	cohesive force
β	the slope of the line fitting the secondary consolidation section

3 NUMERICAL BACK ANALYSIS PLATFORM

Influenced by size effect and the constraints of experiment conditions, the parameters obtained from the laboratory experiment will inevitably lead to large deviation between the calculation result and the monitoring data (Xu et al. 2019). Therefore, in order to improve the accuracy of calculation and prediction, settlement monitoring data was taken as the target and

the parameters of time-dependent UH model were back analyzed by genetic algorithm. The objective function is given as:

$$f = \min \sum_{i=1}^{n} \sum_{j=1}^{m} \left(s_{ij}(\mathbf{p},\ t_j) - s_i(t_j) \right)^2 \tag{8}$$

where i and j are selected monitoring points and monitoring times; $\mathbf{p}$ is a vector of the unknown parameters; $s_i(t_j)$ is the settlement monitoring value of the monitoring point i at the monitoring time j; $s_{ij}(\mathbf{p}, t_j)$ is the corresponding numerical result when the input parameter vector is $\mathbf{p}$.

The finite element software ABAQUS was used for numerical calculation. Therefore, it is necessary to add the call command of ABAQUS to the optimization algorithm, and the time-dependent UH model was written into the user material subroutine (UMAT) embedded in ABAQUS.

4 THE EFFECTIVE PREDICTION INTERVAL METHOD

4.1 The concept of effective prediction interval

After the parameters were determined, the settlement at a certain time in the future can be calculated. However, the accuracy of prediction in the later period decreases. The reason is the monitoring data used to determine parameters is limited. With the increase of time, the error will gradually accumulate. When the error accumulation reaches a certain level, the accuracy and reliability of the predicted settlement will not be guaranteed.

As shown in Fig. 1, based on the settlement monitoring data in the existing measured data interval t_m, the prediction curve is obtained by numerical back analysis.

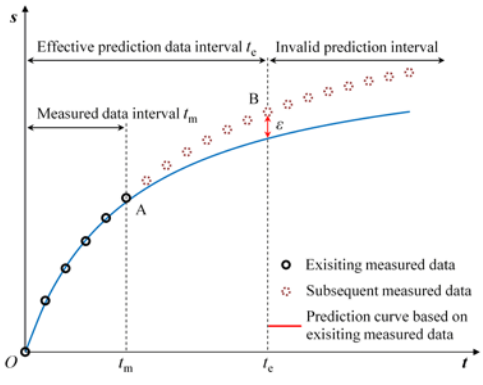


Fig. 1. Concept graph of effective prediction interval for long-term settlement.

As the prediction time increases, the error between the prediction result and the monitoring data is larger and larger. Assume that the subsequent monitoring data reaches the allowed settlement error limit ε at point B, and the corresponding time is the effective prediction time t_e. t_e is called the effective prediction interval corresponding to the measured data interval t_m. The prediction error after t_e is larger than the settlement error limit ε, which does not satisfy the prediction requirement. The time after t_e is called invalid prediction interval.

4.2 Calculation of effective prediction interval

Under a certain settlement error limit ε, a measured data interval t_m determines an effective prediction interval t_e. Generally, the larger the measured data interval t_m, the larger the corresponding effective prediction interval t_e, that is, the longer the monitoring time and the more sufficient the monitoring data, the more accurate the predicted long-term settlement. Therefore, the relationship between t_m and t_e is positively correlated, and $t_e \geq t_m$. t_e/t_m is actually an effective prediction ratio. The relationship between the effective prediction ratio t_e/t_m and t_m is: when t_m is small, the effective prediction ratio t_e/t_m is large; when t_m is large enough, t_e/t_m approaches 1. Therefore, when t_m is sufficiently large, $t_e/t_m=1$ is an asymptote of the t_e/t_m-t_m curve, as shown in Fig. 2.

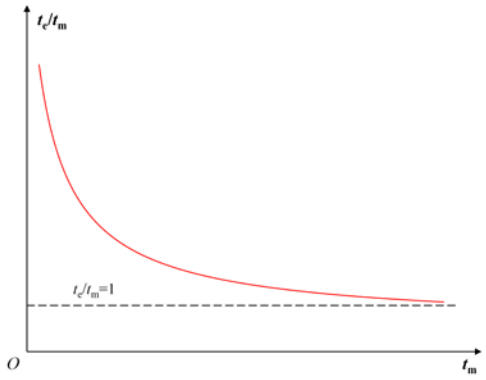


Fig. 2. The curve of t_m-t_e/t_m.

After taking the logarithm of the effective prediction ratio t_e/t_m, the relationship between $\log(t_e/t_m)$ and t_m is: when t_m is sufficiently large, $\log(t_e/t_m)$ approaches 0, i.e. $\log(t_e/t_m)$ is the asymptote of the $\log(t_e/t_m)$-t_m curve. At this time, the relationship between $\log(t_e/t_m)$-t_m and $(t_m/t_0)^{-1}$ is positively correlated:

$$\log\left(t_e/t_m\right) \propto \left(t_m/t_0\right)^{-1} \tag{9}$$

where t_0 is the unit time of the same dimension as t, and the value is 1.

When t_m is small, both $\log(t_e/t_m)$ and $(t_m/t_0)^{-1}$ are large; when t_m is sufficiently large, both $\log(t_e/t_m)$ and $(t_m/t_0)^{-1}$ approach zero. The nonlinear positive correlation between $\log(t_e/t_m)$ and $(t_m/t_0)^{-1}$ can be expressed in the form of a power function. So the relationship between t_e and t_m is established as follows:

$$\log\left(t_e/t_m\right) = \kappa\left(t_m/t_0\right)^{-n} \tag{10}$$

where κ and n are fitting parameters, all being real numbers greater than zero.

The parameters κ and n are determined by the existing settlement monitoring data. If the discreteness of the monitoring data is large, the monitoring data should be smoothed firstly to reduce the background noise. Then the corresponding settlement data on the smooth settlement-time curve is selected to determine the parameters κ and n. Take three sets of data to determine parameters as example, as shown in Fig. 3. Firstly, three measured data interval are selected: t_{m1}, t_{m2}, t_{m3}. Then based on the monitoring data in the respective intervals, three settlement prediction curves can be obtained by numerical calculation. Compare monitoring data with prediction curves based on the settlement error limit ε, and the effective prediction intervals corresponding to the three measured data intervals are obtained: t_{e1}, t_{e2}, t_{e3}. In this way, three sets of (t_m, t_e) are obtained, and the three sets are fitted according to Eq. (10). And then, the fitting parameters κ and n are determined and the fitting curve is drawn, as shown in Fig. 4.

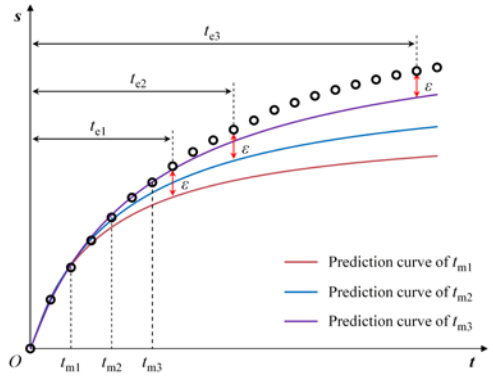


Fig. 3. The determination of t_e.

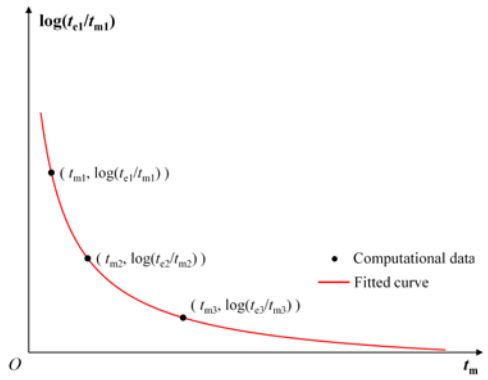


Fig. 4. The curve of t_m-lg(t_e/t_m) based on monitoring data.

The effective prediction interval t_e corresponding to a given measured data interval t_m can be calculated according to Eq. (10) and the determined κ and n. After the monitoring time and the number of monitoring increase, the parameters κ and n need to be re-determined, and the effective prediction interval t_e of the existing measured data interval t_m at a specific settlement error limit ε is re-calculated by the Eq. (10).

5 THE CASE OF CHENGDE AIRPORT

5.1 Introduction of Chengde Airport

Chengde Airport is located in the mountainous area of Chengde City, Hebei Province. The airport construction began in April 2011 and completed in October 2014. The runway of Chengde Airport is 2800m long and spans the excavation area and the filling area. The maximum filling height is 125m, and the total filling amount is 28 million cubic meter. The soil deposit used for the filling is mainly the soil and stone mixture in the excavation area.

The high fill of Chengde Airport is shown in Fig. 5. Two points (i.e., A1, A2 in Fig. 5) in the west wing of the filling area were selected as the settlement monitoring points. The embankment depths of the measurement points were 64, 58m, respectively. The settlement monitoring began on December 21, 2014 and ended on March 29, 2016. A total of 25 times was conducted for a total of 484 days. The settlement curve of each monitoring point is shown in Fig. 6.



Fig. 5. Layout of monitoring points.

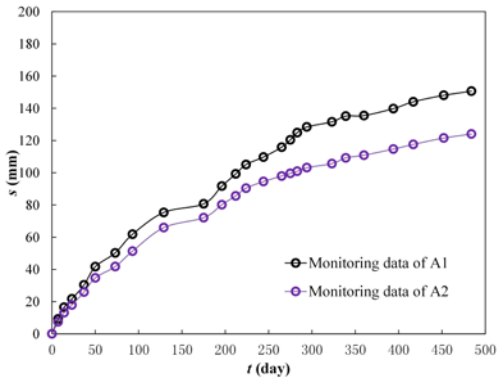


Fig. 6. The values of the monitoring points.

5.2 Effective prediction based on time-dependent UH model

Before the filling starts, the weak geological bodies such as strongly weathered rocks on the original foundation were removed. Therefore, the original foundation is simplified into one layer. In order to reduce the computation amount, the finite element geometric model only established the filling part at the

west end of the runway, as shown in Fig. 8. The vertical displacement and rotation were limited at the bottom, the normal displacement and rotation were limited at the boundary all round. The units were tetrahedral units of C3D4, with a total of 119065 units and 24158 nodes. The finite element model is shown in Fig. 7.

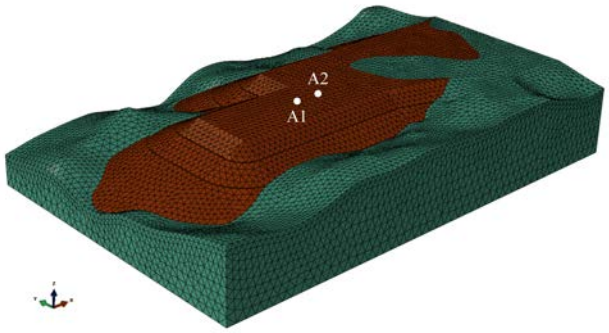


Fig. 7. Finite element mesh model of high fill.

The 323 days of settlement monitoring data from point A1 and A2 were taken as the target for numerical back analysis. The number of parameters in the back analysis is not necessarily the more the better, in especial some complex constitutive models (Sun 2007a; Sun 2007b; Sun 2007c). With the increase of back analysis parameters, there may be some problems such as the increase of calculation amount, the decrease of accuracy and non-unique result. Therefore, the sensitive parameters N and β are selected for back analysis. The other parameters are determined by experience and experiments. The prediction curve based on the monitoring data of 323 days is compared with all the monitoring data of 484 days, as shown in Fig. 8. The parameters of the time-dependent UH model are shown in Table 2.

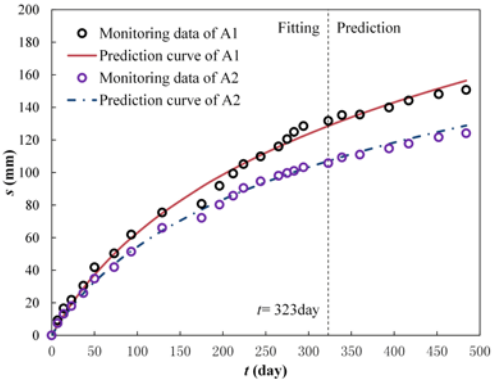


Fig. 8. Predicted curve obtained by numerical back analysis.

Table 2. Parameters of the time-dependent UH model.

Fixed parameters						Parameters to back analysis	
M	μ	κ	λ	e_0	c	N	β
1.2	0.3	0.0098	0.046	0.3	50	0.680	0.00385

It can be seen from Fig. 8 that the finite element calculation based on the time-dependent UH model can well predict the long-term settlement of the high fill of Chengde Airport.

The monitoring data of point A1 and A2 at 14d, 23d, 37d, 50d, 73d, 93d and 129d were taken as the target for back analysis. Taking the settlement error limit ε=5mm and comparing the prediction curve of each group of parameters with the monitoring data, the effective prediction interval t_e of different parameters can be obtained. Due to the discreteness of the monitoring data, the settlement curve of the monitoring points was smoothed. Then the predicted curves were compared with the smoothed curve. Taking t_m=23d, 73d and 129d of point A1 as examples, the process of determination t_e is shown in Fig. 9.

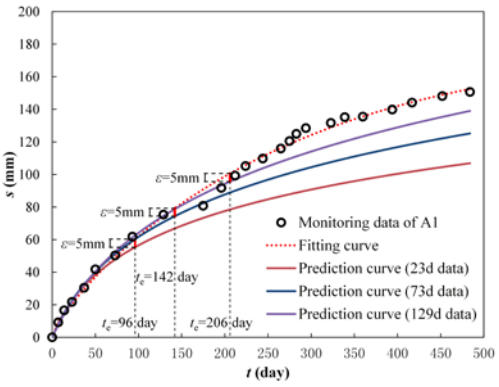


Fig. 9. Determination of t_e based on different prediction curves.

The same method can be used to obtain the effective prediction interval t_e of point A1 and A2 under different measured data interval t_m. The effective prediction interval t_e under different measured data interval t_m is shown in Table 3. The parameters κ and n of the effective prediction interval curve of point A1 and A2 could be got by the least square method, as shown in Table 4. The calculated results of (t_m, lg(t_e/t_m)) of point A1 and A2 and the curves of effective prediction interval are drawn in the same coordinate system, as shown in Fig. 10.

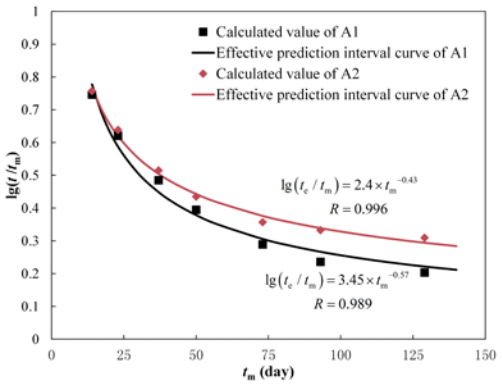


Fig. 10. The t_m-lg(t_e/t_m) curve based on numerical back analysis.

Table 3. The value of t_e under different t_m.

t_m	t_e (d)		lg(t_e/t_m)	
(d)	A1	A2	A1	A2

14	78	80	0.746	0.757
23	96	100	0.621	0.638
37	113	121	0.485	0.515
50	124	136	0.394	0.435
73	142	166	0.289	0.357
93	160	200	0.236	0.333
129	206	263	0.203	0.309

Table 4. The value of fitting parameter κ, n and correlation coefficient R.

Monitoring point	Fitting Parameters		R
	κ	n	
A1	3.45	0.57	0.989
A2	2.40	0.43	0.996

6 CONCLUSIONS

Through the analysis and calculation, the following conclusions are drawn:

(1) The time-dependent UH model proposed by Yao et al. is suitable for calculation and prediction of long-term settlement of high fill after it is embedded in software ABAQUS. Compared with the modified Cam-clay model, this model only adds a parameter, viscosity coefficient β, and all parameters can be determined by laboratory experiments.

(2) When using the numerical calculation based on the time-dependent UH model to predict the long-term settlement of high fill, according to $\log\left(t_e/t_m\right)=\kappa\left(t_m/t_0\right)^{-n}$, the measured data interval t_m can be used to calculate the corresponding effective prediction interval t_e under a specific settlement error limit ε.

ACKNOWLEDGEMENTS

This work was supported by the National Natural Science Foundation of China (Grant No. 11672015, No. 51979001, No. U1834206), the National Program on Key Basic Research Project of China (973 Program, Grant No. 2014CB047000) and the Science and Technology Research and Development Plan of China Railway Corporation (Grant No. 2017G002 - W).

REFERENCES

1) Gao, Z. W., Zhao, J. D. and Yao, Y. P. (2010): A generalized anisotropic failure criterion for geomaterials, *International Journal of Solid and Structures*, 47, (22-23): 3166-3185. (DOI: 10.1016/j.ijsolstr.2010.07.016)
2) Guo, N. and Zhao, J. D. (2013): The signature of shear-induced anisotropy in granular media, *Computers and Geotechnics*, 47: 1-15. (DOI: 10.1016/j.compgeo.2012.07.002)
3) Liu, S. F. and Yang, Y. J. (2015): Advances in Grey System Research(2004-2014), *Journal of Nanjing University of Aeronautics & Astronautics*, 47(01), 1-18. (in Chinese) (DOI: 10.16356/j.1005-2615.2015.01.001)
4) Peng, T., Yang, A. Y., Liang, X. and Yuan, Q. (2005): Prediction of soft ground settlement based on BP neural network-grey system united model, *Rock and Soil Mechanics*, 11:119-123. (in Chinese) (DOI: 10.1007/s11769-005-0030-x)
5) Sridharan, A., Murthy, N. S. and Prakash, K. (1987): Rectangular Hyperbola Method of Consolidation Analysis, *Géotechnique*, 37(3), 355-368. (DOI: 10.1680/geot.1987.37.3.355)
6) Sun, D. A., Sheng, D. C., Cui, H. B. and Sloan, S. W. (2007a): A density-dependent elastoplastic hydro-mechanical model for unsaturated compacted soils, *International Journal for Numerical and Analytical Methods in Geomechanics*, 31(11):1257-1279. (DOI: 10.1002/nag.579)
7) Sun, D. A., Sheng, D. C. and Sloan, S. W. (2007b): Elastoplastic modeling of hydraulic and stress-strain behavior of unsaturated soils, *Mechanics of Materials*, 39(3): 212-221. (DOI: 10.1016/j.mechmat.2006.05.002)
8) Sun, D. A., Sheng, D. C. and Xu, Y. F. (2007c): Collapse behaviour of unsaturated compacted soil with different initial densities, *Canadian Geotechnical Journal*, 44(6): 673-686. (DOI: 10.1139/t07-023)
9) Xu, M., Jin, D. H. and Song, E. X., Shen, Z. P., Yang, Z. J. and Fu, J. Y. (2019): Full-scale creep test and back-analysis of the long-term settlement of heavyloaded shallow foundations on a high rockfill embankment, *Computers and Geotechnics*, 115(11):1-15 (DOI: 10.1016/j.compgeo.2019.103156)
10) Yao, Y. P., Sun, D. A. and Matsuoka, H. (2008a): A unified constitutive model for both clay and sand with hardening parameter independent on stress path, *Computers and Geotechnics*, 35(2): 210-222. (DOI: 10.1016/j.compgeo.2007.04.003)
11) Yao, Y. P., Yamamoto, H. and Wang, N. D. (2008b): Constitutive model considering sand crushing, *Soils and Foundations*, 48(4): 603-608. (DOI: 10.3208/sandf.48.603)
12) Yao, Y. P., Hou, W. and Zhou, A. N. (2009): UH model: three-dimensional unified hardening model for over consolidated clays, *Geotechnique*, 2009, 59(5): 451-469. (DOI: 10.1680/geot.2007.00029)
13) Yao, Y. P., Kong, L. M. and Hu, J. (2013): An elastic-viscous-plastic model for overconsolidated clays, SCIENCE CHINA Technological Science, 56 (2): 441-457. (DOI: 10.1007/s11431-012-5108-y)
14) Yao, Y. P. and Zhou, A. N. (2013): Non-isothermal unified hardening model: a thermo-elasto-plastic model for clays, *Geotechnique*, 63(15): 1328-1345. (DOI: 10.1680/geot.13.P.035)
15) Yao, Y. P., Kong, L. M., Zhou, A. N. and Yin, J. H. (2015): Time-dependent unified hardening model: Three-dimensional elastoviscoplastic constitutive model for clays, *Journal of Engineering Mechanics*, 141(6):04014162. (DOI: 10.1061/(ASCE)EM.1943-7889.0000885)
16) Yao, Y. P., Qi, S. J., Che, L. W., Chen, J., Han, L. M. and Ma, X. Y. (2018a) : Postconstruction settlement prediction of high embankment of silty clay at Chengde airport based on one-dimensional creep analytical method: case study, *International Journal of Geomechanics*, 18(7), 05018004(1-8). (DOI: 10.1061/(ASCE)GM.1943-5622.0001191)
17) Yao, Y. P., Wang, S., Wang, N. D. and Zhang, Q. L. (2018b): Prediction method for long-term settlements of high-speed railway subgrade under influences of nearby loads, *Chinese Journal of Geotechnical Engineering*, 41(4):625-630. (in Chinese) (DOI: 10.11779/CJGE201904004)
18) Zeng, G. X. and Yang, X. L. (1959): Settlement analysis of foundation of sand drain, *Journal of Zhejiang University*, 03:34-72. (in Chinese)